Exploring mechanisms for the decrease of atmospheric CO_2 during the last glacial maximum using a four-box ocean model

by

Stacey A. Archfield

Submitted to the Department of Earth, Atmospheric, and Planetary Sciences
in Partial Fulfillment of the Requirements for the Degree of
Master of Science
at the

Massachusetts Institute of Technology

June 2001

Author .....
Department of Earth, Atmospheric, and Planetary Sciences
May 4, 2001

Certified by .....
Edward A. Boyle
Professor of Marine Geochemistry
Thesis Supervisor

Accepted by .....
Dale Morgan
Director, Geosystems Program

Accepted by ....
Ronald G. Prinn
Head, Department of Earth, Atmospheric and Planetary Scienes

Exploring mechanisms for the decrease of atmospheric CO_2 during the last glacial maximum using a four-box ocean model

by

Stacey A. Archfield

Submitted to the Department of Earth, Atmospheric, and Planetary Sciences
on May 30, 2001 in Partial Fulfillment of the Requirements
for the Degree of Master of Science

Abstract

A record of carbon dioxide for the last 400,000 years revealed that atmospheric CO_2 decreased from a pre-industrial concentration of 280 ppmV to approximately 200 ppmV during the last glacial maximum (Petit et al., 1999). Several hypotheses as to why this happened have been suggested yet no one explanation has been able to fully account for this decrease. Deep water is the main sink for carbon in the ocean through the biological pump, where the organic matter and $CaCO_3$ shells of dead surface biota sink. The stored carbon in the deep ocean is 'aired' in the southern polar ocean, where large amounts of deep water are upwelled to the surface. Stephens and Keeling (2000) have proposed that if the southern polar ocean was covered with ice during the last glacial maximum, this would have prevented carbon stored in the deep ocean to be released into the atmosphere, thereby reducing the concentration of atmospheric CO_2. Stephens and Keeling (2000) created a six-box ocean to test this hypothesis and were able to produce a 67 ppmV decrease of atmospheric CO_2 from the pre-industrial concentration when only the gas exchange between the southern polar ocean and the atmosphere was limited. Based on the Toggweiler and Sarmiento (1985) three-box ocean model, a four-box ocean model that splits the Toggiweiler and Sarmiento polar ocean box in to a northern and southern component was created. The four-box ocean model examined the sensitivity of atmospheric CO_2 to limitations in the air-sea gas exchange for the southern polar ocean. The four-box ocean was able to produce seventy percent of Stephens and Keeling's decrease in atmospheric CO_2 when the air-sea gas exchange was limited in the southern polar ocean. In addition, the four-box ocean model calculated carbon-14 concentrations in the ocean, which provide a useful constraint on model results that was not presented in the Stephens and Keeling model. The atmospheric carbon dioxide in the four box model was found to be more sensitive to increasing biological productivity in the southern polar ocean than to the growth of the Antarctic ice sheet.

Thesis Supervisor: Edward A. Boyle

Title: Professor of Marine Geochemistry

Table of Contents

List of Figures and Tables

I. Introduction

One hundred years ago, the pre-industrial concentration of carbon dioxide in the atmosphere was approximately 280 parts per million by volume (ppmV) (Petit et al., 1999). About 18,000 years ago, at the last glacial maximum, the concentration of atmospheric CO_2 was between 180 and 200 ppmV (Petit et al., 1999). The cause of this 80 ppmV decrease in atmospheric CO_2 has yet to be explained. Several hypotheses have been suggested, yet no one explanation has been able to fully account for this decrease. Sigman and Boyle (2000) have presented these different hypotheses in a review article.

Despite the differing hypotheses about the mechanism that caused atmospheric CO_2 to decrease during the last glacial maximum, almost all hypotheses point to changes in the behavior of the ocean as the cause. The ocean utilizes a 'biological pump' where carbon is sequestered in the deep ocean through a particulate flux of carbon created by the sinking of organic matter and $CaCO_3$ shells from dead surface organisms (Sigman and Boyle, 2000). The deepest layers of the ocean are responsible for large-scale CO_2 regulation through these particulate fluxes of organic and carbonate particles from the warm surface ocean to the deep (Siegenthaler and Wenk, 1984). Since the deep waters of the ocean are exposed every 1000 years, the ocean serves as the largest of carbon reservoirs and controls atmospheric CO_2 on time scales of less than 10^5 years (Siegenthaler and Wenk, 1984).

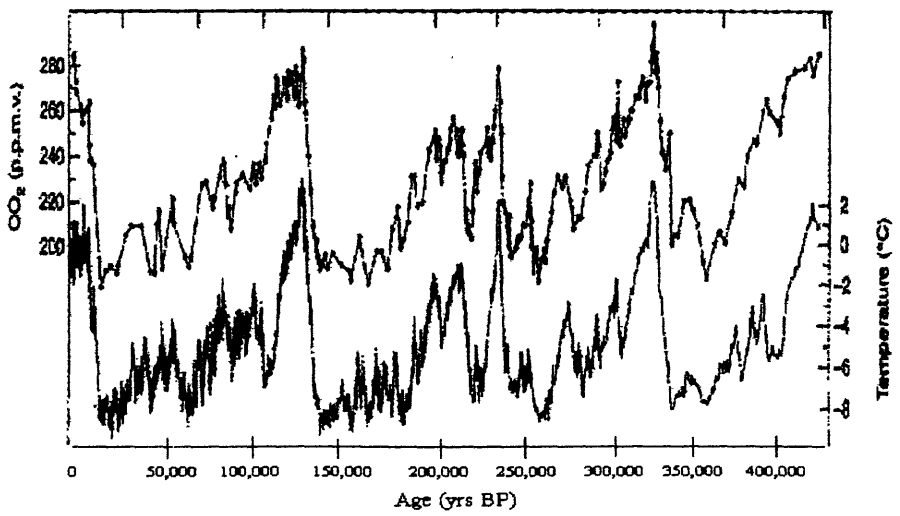

Figure 1: Record of temperature anomalies and carbon dioxide for the last 400,000 years. (Petit et al., 1999).

The measurements from Petit et al. have shown that there is a relationship between changes in temperature and changes in atmospheric carbon dioxide for the last 400,000 years (Petit et al, 1999). Figure 1 shows this relationship between temperature and CO_2.

In addition figure 1 shows that CO_2 and temperature follow a cyclic pattern with a period of 100,000 years. Temperature decreases every 100,000 years can be explained by the Milankovich cycles and feedbacks associated with those cycles. However, since CO_2 and temperature are closely related and CO_2 is currently increasing due to biomass burning and the burning of fossil fuels, it is important that we gain an understanding of the factors controlling long-term atmospheric CO_2 concentrations.

II. Background: Ocean Circulation, Antarctic Sea Ice and Atmospheric CO_2

Large-scale ocean circulation has been described as a 'conveyor-belt' pattern (Broecker, 1991). In the north polar ocean, surface water becomes dense enough to sink due to decreased temperature and increased salinity. As the denser water sinks, it is replaced by pole-ward moving water rising from immediate depths (Broecker, 1991). The dense North Atlantic Deep Water (NADW) moves southward along the ocean bottom, where it upwells in the South Polar Ocean (Broecker, 1991). This upwelling in the southern polar ocean is responsible for the airing of the deep waters of the ocean by exposing large quantities of this water to the atmosphere (Broecker, 1991).

Stephens and Keeling (2000) suggest that if the southern polar ocean were covered with sea ice during the last glacial maximum, it would have limited the amount of CO_2 released from the deep ocean into the atmosphere thereby reducing the amount of atmospheric CO_2 'leaking' out of the biological pump. This investigation will focus on testing this hypothesis via the construction of a four-box ocean model and will analyze the effects of limiting air-sea gas exchange in the southern polar ocean. The results will then be compared to Stephens and Keeling's result from their six-box ocean model. The four-box ocean model will also extend Stephens and Keeling's calculations to look at the sensitivity of carbon-14 to limiting gas exchange in the southern polar ocean. Carbon-14 can provide a useful constraint on model results due to its ability to provide relative ages for different areas of the ocean.

III. Statement of the Problem

Develop a four-box model of the ocean and atmosphere to explore the sensitivities of the following parameters to the growth of the Antarctic ice sheet as a mechanism to explain the decrease of atmospheric CO_2 during the last glacial maximum:

1. Atmospheric carbon dioxide
2. High-latitude southern ocean surface water $\delta^{13}C$ concentration
3. Deep water O_2 concentration
4. $\Delta^{14}C$ concentration of the atmosphere, deep ocean and southern polar ocean
5. $\Delta^{14}C$ age of the deep ocean and the warm surface ocean

IV. Methodology

A four-box ocean model was developed based on the Toggweiler and Sarmiento three-box ocean model to test the hypothesis of Stephens and Keeling. The Toggweiler and Sarmiento three-box ocean model combined the southern and northern polar oceans into one box. However, when the piston velocity was reduced in the polar box to simulate growth of the ice sheets, atmospheric CO_2 was not sensitive to these changes. Figure 2 shows the structure of the Toggweiler and Sarmiento three-box model. Open arrows indicate water fluxes between each box, solid arrows indicate particulate fluxes from the surface boxes to the deep ocean and dashed lines indicate gas fluxes when the ocean is coupled with the atmosphere.

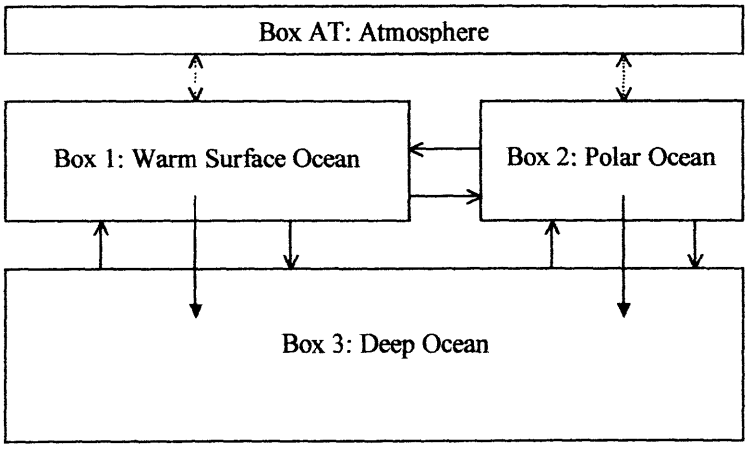

Figure 2: Toggweiler and Sarmiento (1985) three-box ocean .Model

To circumvent the problem with the three-box model, a four-box ocean model was created to separate the polar ocean into two boxes: a high-latitude northern ocean and a high-latitude southern ocean. Figure 3 shows the divisions of the ocean into four boxes. As in figure 2, open arrows indicate water fluxes between each box, solid arrows indicate particulate fluxes from the surface boxes to the deep ocean and dashed lines indicate gas fluxes when ocean is coupled with the atmosphere.

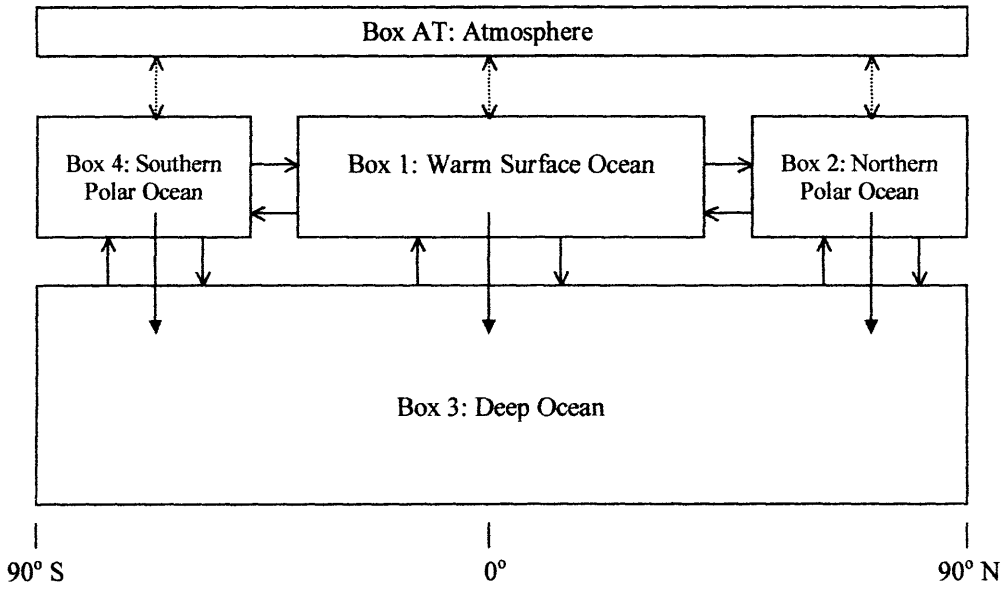

Figure 3: Four-box ocean model

To simulate the growth of the Antarctic ice sheet, the air-sea gas exchange was limited in the high-latitude southern ocean by decreasing the piston velocity. The sensitivities of atmospheric carbon dioxide to varying amounts of gas exchange limitations were explored. In addition, model sensitivity to air-sea gas exchange was also tested for deep O_2, high latitude southern ocean $\delta^{13}C$ concentration and $\Delta^{14}C$.

V. Construction of the Four-Box Ocean Model

Through the equations and approach used in the Toggweiler and Sarmiento (1985), Siegenthaler and Wenk (1984), and Knox and McElroy (1984) models, the four-box ocean model calculates, in order, the following constituents listed below. The model is designed such that each of the constituents is dependent on the constituents previously

solved for in the model. For example, carbon dioxide is dependent on salinity, temperature, phosphorus and alkalinity. However, the solutions for carbon dioxide are not dependent on the values for carbon-13, carbon-14, and oxygen. For each of these constituents, an explanation of the methodology is described in further detail.

1. Salinity and Temperature
2. Phosphorus
3. Alkalinity
4. Total Carbon and Carbon Dioxide
5. Carbon-13
6. Carbon-14
7. Oxygen

1. Salinity and Temperature

The water fluxes between each box are defined and a flux of water is also included that accounts for moisture flux from low latitudes which results in precipitation at higher latitudes (Broecker, 1991). This additional flux allows for a more realistic salinity distribution, where the high latitude ocean boxes are less salty than the low latitude box. Using the water fluxes and mass balance, the salinity is solved for using simultaneous equations that have been presented in matrix format, as shown in equation (1). Since salinity is conservative, note that row three of the matrix is a mass balance equation.

$$\begin{bmatrix} -(Q_{14}+Q_{13}+Q_{12}) & Q_{21} & Q_{31} & Q_{41} \\ Q_{12} & -(Q_{21}+Q_{23}) & Q_{32} & 0 \\ V_1 & V_2 & V_3 & V_4 \\ Q_{14} & 0 & Q_{34} & -(Q_{41}+Q_{43}) \end{bmatrix} \begin{bmatrix} S_1 \\ S_2 \\ S_3 \\ S_4 \end{bmatrix} = \begin{bmatrix} 0 \\ 0 \\ S_{total} \\ 0 \end{bmatrix} \quad (1)$$

$$\boldsymbol{A} \qquad\qquad \boldsymbol{x} \qquad \boldsymbol{b}$$

where: Q_{ab} = flux of water from box a to box b
S_a = concentration of salinity in box a
S_{total} = total amount of salt in the ocean
V_a = volume of water in box a

A = water flux exchanges between the four boxes
x = concentration of salinity in each of the four boxes
b = fluxes not accounted for in the A matrix
$x = A^{-1}b$

Since water fluxes in and out of each box are defined, temperature is merely assigned in this portion of the model and is not a parameter that is solved for. These temperature values will be used later in the model when the ocean is coupled with an atmosphere and gas solubility is calculated.

2. *Phosphorus*

Since the observational values are better known for phosphorus than for particulate fluxes, the concentrations of phosphorus in the surface boxes are assigned and the particulate flux of phosphorus from the surface boxes to the deep ocean is solved for using mass conservation and simultaneous equations. The A matrix contains the same fluxes used to solve for salinity. However, since there are now particulate fluxes in addition to the water fluxes, the b matrix no longer contains zeroes and these particulate fluxes have been placed there. Equation (2) illustrates these equations. Since phosphorus is also conserved, row three of the matrices is a mass balance equation.

$$\begin{bmatrix} -(Q_{14}+Q_{13}+Q_{12}) & Q_{21} & Q_{31} & Q_{41} \\ Q_{12} & -(Q_{21}+Q_{23}) & Q_{32} & 0 \\ V_1 & V_2 & V_3 & V_4 \\ Q_{14} & 0 & Q_{34} & -(Q_{41}+Q_{43}) \end{bmatrix} \begin{bmatrix} P_1 \\ P_2 \\ P_3 \\ P_4 \end{bmatrix} = \begin{bmatrix} PF_{P13} \\ PF_{P23} \\ P_{total} \\ PF_{P43} \end{bmatrix} \qquad (2)$$

$$\boldsymbol{A} \qquad\qquad \boldsymbol{x} \qquad \boldsymbol{b}$$

where: P_a = concentration of phosphorus in box a
P_{total} = total amount of phosphorus in the ocean
PF_{Pa3} = particulate flux of phosphorus from box a to box 3
$b = Ax$

3. *Alkalinity*

The total alkalinity and normalized alkalinity is calculated as well as the particulate flux of alkalinity to the deep ocean using the Redfield ratio of alkalinity to

phosphorus suggested in the Toggweiler and Sarmiento model. The concentration of alkalinity is solved for using the same technique as salinity. Equation (3) presents these equations.

$$\begin{bmatrix} -(Q_{14}+Q_{13}+Q_{12}) & Q_{21} & Q_{31} & Q_{41} \\ Q_{12} & -(Q_{21}+Q_{23}) & Q_{32} & 0 \\ V_1 & V_2 & V_3 & V_4 \\ Q_{14} & 0 & Q_{34} & -(Q_{41}+Q_{43}) \end{bmatrix} \begin{bmatrix} AL_1 \\ AL_2 \\ AL_3 \\ AL_4 \end{bmatrix} = \begin{bmatrix} PF_{AL13} \\ PF_{AL23} \\ AL_{total} \\ PF_{AL43} \end{bmatrix} \quad (3)$$

$$\boldsymbol{A} \qquad\qquad \boldsymbol{x} \qquad \boldsymbol{b}$$

where: AL_a = concentration of phosphorus in box a
AL_{total} = total amount of phosphorus in the ocean
PF_{ALa3} = particulate flux of phosphorus from box a to box 3
$= (PF_{Pa3})(RedfieldRatio_{ALa})$
$x = A^{-1}b$

The normalized alkalinity was calculated using equation (4):

$$NA = \frac{35 \times AL_a}{S_a} \quad (4)$$

Since variations in alkalinity are mainly due to changes in salinity, calculating the normalized alkalinity provides a way to confirm that the model calculations for alkalinity are consistent with the solutions for salinity in each box (Chester, 1990).

4. Total Carbon and Carbon Dioxide

Carbon dioxide is transported through the atmosphere, so the four-box ocean model is now coupled with an atmosphere. Furthermore, since carbon dioxide is not related to alkalinity by a linear relationship, iteration must be used to solve for the concentration of total inorganic carbon in the ocean based on the solubility of carbon dioxide and the gas fluxes between the surface boxes and the atmosphere (Toggweiler and Sarmiento, 1985). The iteration process guesses the concentration of carbon dioxide in the atmosphere based on the gas fluxes in and out of each surface box and

continues until a solution converges. Since the gas fluxes are dependent on the concentration of carbon dioxide in the atmosphere and the solubility of carbon dioxide in the surface ocean boxes (which is, in turn, dependent on temperature), the following calculations are performed in each iteration until a solution converges:

1. Initial gas fluxes for each surface box are chosen. Total inorganic carbon in each of the surface boxes is solved for through equation (5). Carbon is conservative, so a mass balance equation is used in row three of the matrices.

$$\underbrace{\begin{bmatrix} -(Q_{14}+Q_{13}+Q_{12}) & Q_{21} & Q_{31} & Q_{41} \\ Q_{12} & -(Q_{21}+Q_{23}) & Q_{32} & 0 \\ V_1 & V_2 & V_3 & V_4 \\ Q_{14} & 0 & Q_{34} & -(Q_{41}+Q_{43}) \end{bmatrix}}_{\boldsymbol{A}} \underbrace{\begin{bmatrix} \Sigma CO_{21} \\ \Sigma CO_{22} \\ \Sigma CO_{23} \\ \Sigma CO_{24} \end{bmatrix}}_{\boldsymbol{x}} = \underbrace{\begin{bmatrix} PF_{C13}+GF_1 \\ PF_{C23}+GF_2 \\ C_{total}-(pCO_{2_{AT}} \times V_{AT_{total}}) \\ PF_{C43}+GF_4 \end{bmatrix}}_{\boldsymbol{b}} \quad (5)$$

where: $\Sigma CO_{2\,a}$ = concentration of inorganic carbon in box *a*
C_{total} = total amount of carbon in the ocean
PF_{Pa3} = particulate flux of carbon from box *a* to box 3
GF_a = gas flux between box *a* and the atmosphere
$pCO_{2\,AT}$ = concentration of CO_2 in the atmosphere
$V_{AT\,total}$ = total volume of the atmosphere
$x = A^{-1}b$

NOTE: The carbon particulate flux was calculated using the Redfield Ratio for organic carbon to phosphorus as suggested in the Toggweiler and Sarmiento (1985) model. The Redfield ratio of total inorganic carbon was then calculated from equation (6):

$$RR_{\Sigma CO_2} = RR_{organicC} + \left(\frac{AL_a}{2}\right) \quad (6)$$

2. The program guesses a value for atmospheric carbon dioxide.

3. Gas fluxes for each surface box are calculated using the formula (Pilson, 1998):

$$GF_a = Area_a \times PV_a \times \left(CO_{2_a} - \left(pCO_{2_{AT}} \times \alpha_a\right)\right) \quad (7)$$

where: PV_a = piston velocity for box *a*
$CO_{2\,a}$ = concentration of dissolved CO2 in box *a*
α_a = equilibrium constant of solubility for box *a*

4. The midpoint of the initial gas flux and the calculated gas flux for each box is calculated.
5. The midpoint of each surface flux is used to determine the new gas flux that will be input back into Step 1. Since the difference between the initial gas fluxes and the calculated fluxes can be very large, the new gas flux values inserted into Step 1 for the next iteration are changed by only 10% of the midpoint to insure a smooth convergence. Equation (8) illustrates this calculation:

$$NewGasFlux_a = (0.1 \times Midpt_a) + (0.9 \times ValuefromStep1_a) \quad (8)$$

6. The iteration process continues until the calculated midpoint between each of the gas fluxes is less than 0.0001.

5. Carbon-13

Since the gas flux of carbon dioxide is calculated through the iteration process, it is possible to derive the fraction of total inorganic carbon and carbon dioxide that is carbon-13. The gas fluxes in and out of the atmosphere for each box are than calculated using equations (9) and (10):

Flux out of the atmosphere into box *a* (Broecker and Peng, 1982):

$$GF_{ATa} = Area_a \times (KineticEffect_{13_C} \times PV_a) \times \alpha_{13_a} \quad (9)$$

Flux into atmosphere from box *a* (Broecker and Peng, 1982):

$$GF_{aAT} = Area_a \times (KineticEffect_{13_C} \times PV_a) \times frac_{13_{C\,(aq)}} \quad (10)$$

where: $KineticEffect_{13C}$ = effect due to isotopic substitution
$frac_{13C(aq)}$ = fraction of dissolved CO_2 which is $^{13}CO_2$
α_a = equilibrium constant of solubility for box *a*

Then, $\Sigma\ ^{13}CO_2$ is solved for using equation (11), with the atmosphere now being treated as an additional box.

$$\underbrace{\begin{bmatrix} -(Q_{14}+Q_{13}+Q_{12}+GF_{1AT}) & Q_{21} & Q_{31} & Q_{41} & GF_{AT1} \\ Q_{12} & -(Q_{21}+Q_{23}+GF_{2AT}) & Q_{32} & Q_{42} & GF_{AT2} \\ Q_{13} & Q_{23} & -(Q_{32}+Q_{31}+Q_{34}) & Q_{43} & 0 \\ Q_{14} & 0 & Q_{34} & -(Q_{41}+Q_{43}+GF_{4AT}) & GF_{AT4} \\ V_1 & V_2 & V_3 & V_4 & V_{AT} \end{bmatrix}}_{A} \underbrace{\begin{bmatrix} \Sigma^{13}CO_{21} \\ \Sigma^{13}CO_{22} \\ \Sigma^{13}CO_{23} \\ \Sigma^{13}CO_{24} \\ p^{13}CO_{2_{AT}} \end{bmatrix}}_{x}$$

$$= \underbrace{\begin{bmatrix} PF_{^{13}C_{13}} \\ PF_{^{13}C_{23}} \\ -PF_{^{13}C_{14}} - PF_{^{13}C_{23}} - PF_{^{13}C_{43}} \\ PF_{^{13}C_{43}} \\ {}^{13}C_{total} \end{bmatrix}}_{b} \quad (11)$$

where: $\Sigma^{13}CO_{2\,a}$ = concentration of inorganic carbon in box *a*
$^{13}C_{total}$ = total amount of carbon-13 in the ocean
$PF_{13C\,a3}$ = particulate flux of carbon-13 from box *a* to box 3
GF_{ab} = gas flux between box *a* and box *b*
$p^{13}CO_{2\,AT}$ = concentration of $^{13}CO_2$ in the atmosphere
A = water fluxes and gas fluxes between boxes
x = concentration of $\Sigma^{13}CO_{2\,a}$ in each box
b = additional fluxes not included in *A*
$x = A^{-1}b$

$\delta\ ^{13}C$ was also calculated using equation (12) (Broecker and Peng, 1982):

$$\delta^{13}C = \left(\frac{(^{13C/12C})\text{Sample}}{(^{13C/12C})\text{Standard}} - 1 \right) \times 1000 \quad (12)$$

6. Carbon-14

Carbon-14 is solved for in much of the same way as the carbon-13 portion of the model. However, carbon-14 is not conservative. Cosmic rays produce carbon-14 and then the carbon-14 is transported through the atmosphere and into the ocean. In addition to production, carbon-14 is also decaying as it is circulated through the ocean and is therefore able to provide an age constraint to the model. Decay and production

of carbon-14 are treated as an additional flux out of the atmosphere and ocean and are included in the A matrix in equation (14). This additional flux, which is the amount of carbon-14 that is not transported and decays in each box is given by equation (13):

$$D_a = \lambda_{14_C} \times V_a \quad (13)$$

where: λ_{14C} = decay constant for carbon-14

Gas fluxes are calculated from equations (9) and (10) using the kinetic effect (KE_{14}) and the solubility constants (α_{14}) for carbon-14.

$$\underbrace{\begin{bmatrix} -(Q_{14}+Q_{13}+Q_{12}+GF_{1AT}+D_1) & Q_{21} & Q_{31} & Q_{41} & GF_{AT1} \\ Q_{12} & -(Q_{21}+Q_{23}+GF_{2AT}+D_2) & Q_{32} & Q_{42} & GF_{AT2} \\ Q_{13} & Q_{23} & -(Q_{32}+Q_{31}+Q_{34}+D_3) & Q_{43} & 0 \\ Q_{14} & 0 & Q_{34} & -(Q_{41}+Q_{43}+GF_{4AT}+D_4) & GF_{AT4} \\ GF_{1AT} & GF_{2AT} & 0 & GF_{4AT} & -(GF_{AT1}+GF_{AT2}+GF_{AT4}+D_{AT}) \end{bmatrix}}_{A}$$

$$\underbrace{\begin{bmatrix} \Sigma^{14}CO_{21} \\ \Sigma^{14}CO_{22} \\ \Sigma^{14}CO_{23} \\ \Sigma^{14}CO_{24} \\ p^{14}CO_{2_{AT}} \end{bmatrix}}_{x} = \underbrace{\begin{bmatrix} PF_{14C_{13}} \\ PF_{14C_{23}} \\ -PF_{14C_{14}} - PF_{14C_{23}} - PF_{14C_{43}} \\ PF_{14C_{43}} \\ {}^{14}C_{production} \end{bmatrix}}_{b} \quad (14)$$

where: $\Sigma^{14}CO_{2\,a}$ = concentration of inorganic carbon in box a
$^{14}C_{total}$ = total amount of carbon-14 in the ocean
$PF_{14C\,a3}$ = particulate flux of carbon-14 from box a to box 3
D_a = amount of ^{14}C that has decayed in box a
$p^{14}CO_{2\,AT}$ = concentration of $^{14}CO_2$ in the atmosphere
$x = A^{-1}b$

$\delta^{14}C$ and $\Delta^{14}C$ are also calculated using equation (15) and (16) (Broecker and Peng, 1982):

$$\delta^{14}C = \left(\frac{(^{14}C/C)\text{Sample} - (^{14}C/C)\text{Standard}}{(^{14}C/C)\text{Standard}} \right) \times 1000 \quad (15)$$

$$\Delta^{14}C = \delta^{14}C - 2(\delta^{13}C + 25) \times (1 + \delta^{14}C) \quad (16)$$

7. Oxygen

To explore the effects of limiting air-sea gas exchange on deep ocean O_2 concentrations, this portion of the model is also coupled with an atmosphere by calculating the solubility of oxygen in seawater and the piston velocity for oxygen and then solving for the concentration of oxygen in each box. Oxygen is also conserved. However, since the reservoir of oxygen in the atmosphere so large, the concentration of oxygen in the atmosphere can be considered constant. Oxygen is solved for in equation (17). The Redfield ratio of oxygen to phosphorus used in equation (17) to calculate the particulate flux of oxygen is the value suggested by Broecker (1985). Gas fluxes are calculated from equations (9) and (10) but using the piston velocity and solubilities for oxygen:

$$\underset{A}{\begin{bmatrix} -(Q_{14}+Q_{13}+Q_{12}+GF_{1AT}) & Q_{21} & Q_{31} & Q_{41} \\ Q_{12} & -(Q_{21}+Q_{23}+GF_{2AT}) & Q_{32} & 0 \\ Q_{13} & Q_{23} & -(Q_{31}+Q_{32}+Q_{34}) & Q_{43} \\ Q_{14} & 0 & Q_{34} & -(Q_{41}+Q_{43}+GF_{4AT}) \end{bmatrix}} \underset{x}{\begin{bmatrix} O_{21} \\ O_{22} \\ O_{23} \\ O_{24} \end{bmatrix}} = \underset{b}{\begin{bmatrix} -PF_{O13}-GF_{AT1} \\ -PF_{O23}+GF_{AT2} \\ -(PF_{O13}+PF_{O23}+PF_{O43}) \\ -PF_{O43}+GF_{AT4} \end{bmatrix}} \quad (17)$$

where: O_{2a} = concentration of oxygen in box a
$^{14}C_{total}$ = total amount of carbon-14 in the ocean
$PF_{O2\,a3}$ = particulate flux of oxygen from box a to box 3
$x = A^{-1}b$

VI. Stephens and Keeling's Model and Results

Stephens and Keeling suggest that almost of all of the 80 ppmV decrease of atmospheric CO_2 during that last glacial period was due to the growth of sea ice in the high-latitude southern ocean which limited air-sea gas exchange and thus prevented the deep ocean 'airing' of CO_2 (Stephens and Keeling, 2000). Furthermore, Stephens and Keeling (2000) hypothesize that decreasing air-sea gas exchange also produces values for deep oxygen and Antarctic surface $\delta^{13}C$ which correspond to observational data during the last glacial period. They constructed a six-box ocean model coupled with an atmosphere to illustrate this hypothesis using the assumptions that there were no changes in nutrient concentrations and utilization during the last glacial period and that deep waters only return to the surface in the high-latitude southern ocean (Stephens and Keeling, 2000). Stephens and Keeling's (2000) model construction is presented in figure 4 with their solution for pre-industrial conditions in the ocean and atmosphere.

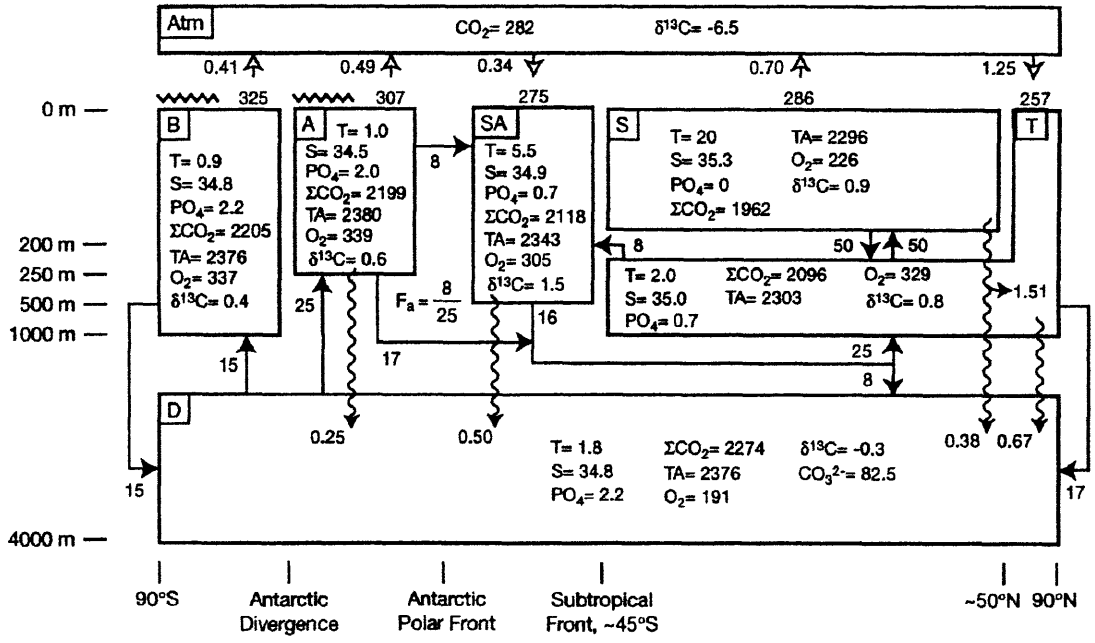

Figure 4: Six-box ocean model developed by Stephens and Keeling and their solutions for a pre-industrial ocean and atmosphere. Box *S* represents the warm surface ocean, box *T* is the main thermocline box, box *SA* represent the southern sub-Antarctic surface ocean, and box *D* represents the deep ocean. F_a is the fraction of northward-flowing water that is exposed to the surface or carried to the deep ocean. Carbon fluxes are in Gt C/yr, concentrations are in μmol/kg except δ13C, which is measured in per mil, temperature is measured in °C, and salinity in psu. Note that box *S* does not communicate directly with box *SA*, *A*, or *B*. In addition, there is no upwelling of deep water except to boxes *B* and *A (from Stephens and Keeling, 2000)*.

Using their six-box ocean model, Stephens and Keeling (2000) were able to produce a decrease of 67 ppmV of atmospheric CO_2. They attribute 92% of this decrease to the reduction of gas exchange in the high-latitude southern ocean and 1.8% of the decrease to an increase in the deep ocean inorganic carbon concentration (Stephens and Keeling, 2000). Stephens and Keeling also found that deep O_2 is not sensitive to these air-sea limitations except when sea ice coverage is very large (2000). Their sensitivities of Antarctic surface $\delta^{13}C$, deep O_2 and atmospheric CO_2 to limitations in the gas exchange are shown in figure 5.

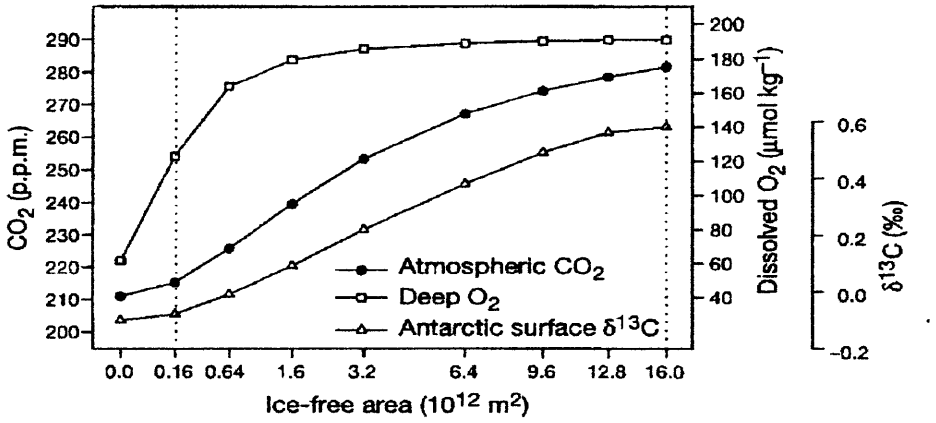

Figure 5: Sensitivities of Stephens and Keeling's six-box ocean model to sea ice coverage in the high-latitude polar ocean. The dotted line on the left represents Stephens and Keeling's estimate for southern ocean ice coverage at the last glacial maximum. The dotted line on the right denotes their pre-industrial values before sea ice coverage was increased (*from Stephens and Keeling, 2000*).

VII. Designation of Values for Four-Box Ocean Model

As a first effort to test Stephens and Keeling's hypothesis, the values used in their model were translated to the four-box ocean model. However, their model had been designed in such a way that the high-latitude northern ocean box communicates with the high-latitude southern ocean box independent of the low-latitude surface box. The four-box ocean model cannot account for this behavior and thus yielded unreasonable results. Furthermore, Stephens and Keeling's (2000) model was also designed to test the sensitivity of their model to northward flowing Antarctic surface waters as it forms deep

water or continues along the surface. Therefore, the values used in their model design were not easily transferable to the four-box ocean model.

Values were then assigned to the four-box ocean model based on the Toggweiler and Sarmiento three-box model but in the 'spirit' of Stephens and Keeling, where low-latitude upwelling from deep water is minimized. Appendix A lists the values for the constants used in the model. The Toggweiler and Sarmiento (1985) three-box model defines a water flux, T, which describes the 'conveyor belt' flux, and water fluxes which exchange between each box. Figure 6 shows Toggweiler and Sarmiento's water flux values for a pre-industrial ocean with $T = 19$ Sv.

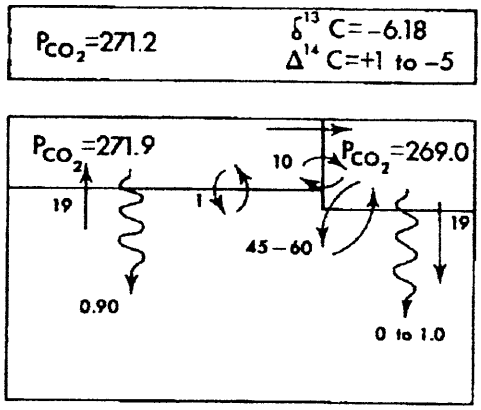

Figure 6: Water flux values used by Toggweiler and Sarmiento in their three-box model of the ocean. Wavy arrows indicate particulate fluxes to the deep ocean. Solid straight arrows represent T, the 'conveyor' flux, and curved arrows indicate the net water flux exchange between the two boxes, excluding T. All water fluxes are in Sv. (Toggweiler and Sarmiento, 1985)

For the three-box model's pre-industrial solution shown in figure 6, a 'conveyor belt' flux of 19 Sv was used. For the four-box ocean model, a slightly lower conveyor flux was used to produce a solution for the modern pre-industrial ocean. The exchange fluxes from Toggweiler and Sarmiento's polar box were split into the northern and southern polar ocean for the four-box model under the assumption that the net water fluxes between the deep ocean and each of the polar boxes would each equal 14 Sv. In addition, Stephens and Keeling's assumption that the amount of upwelling from the deep ocean to the warm surface ocean is minimal was utilized by allowing no net flux of water between those two boxes in the four-box ocean model. Figure 7 shows the fluxes and

initial conditions used to calculate the four-box model solution for the modern pre-industrial ocean.

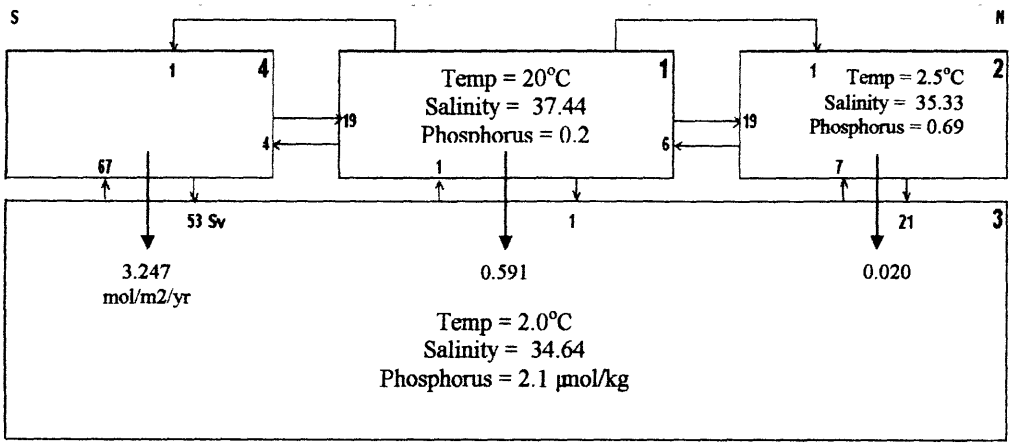

Figure 7: Water fluxes used to calculate the solution for the modern pre-industrial ocean. A conveyor flux of 14 Sv was used. The larger numbers in the right corner of each box denotes the box number. Box 1 is the warm surface ocean, Box 2 is the northern polar ocean, Box 3 is the deep ocean and Box 4 is the southern polar ocean. Solid arrows indicate the particulate flux of carbon. Note that the net flux between Box 4 and Box 3 as well as between Box 2 and Box 3 equals 14 Sv. The atmospheric CO_2 concentration for these conditions is 275 ppmV

As a check to make sure the four-box ocean behaved correctly in response to changes in the rate of ocean overturning, the sensitivity of atmospheric CO_2 and the carbon-14 age of the deep ocean to the speed of the 'conveyor belt' were tested. The results are shown in figure 8.

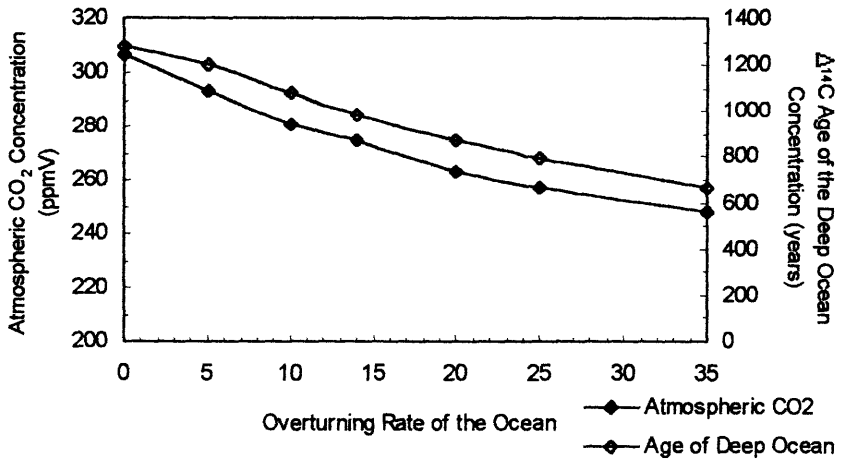

Figure 8: Sensitivity of atmospheric CO_2 and $\Delta^{14}C$ age of the deep ocean to changes in the overturning rate. As expected, when the overturning increases, the residence time of deep water decreases. As overturning increases, the ocean also becomes a more efficient sink for CO_2 and decreases its concentration in the atmosphere.

Appendix B shows the steady-state solutions of the four-box ocean model for the modern pre-industrial ocean; these solutions agree well with observational data. Table 1 is a comparison of observational data to the four-box model prediction of a pre-industrial ocean. Table 1 was constructed as another verification that the model was behaving correctly. Although the purpose of this study was to observe the qualitative behavior of atmospheric CO_2, model output was compared with observational data to ensure the sensitivity tests would produce reasonable values.

Table 1: Comparison of observation data to the four-box ocean model for the modern pre-industrial ocean.

Parameter	Observational Value	Four-Box Ocean Model Output	Reference
Southern Polar Ocean $\Delta^{14}C$	-158 ‰	-160 ‰	Broecker, Virgilio, and Peng (1991)
Northern Polar Ocean $\Delta^{14}C$	-68 ‰	-54 ‰	Broecker, Virgilio, and Peng (1991)
Atmospheric $\Delta^{14}C$	0 ‰	30.55 ‰	Broecker and Peng (1982)
Deep Ocean $\Delta^{14}C$	-141 ‰	-141 ‰	Toggweiler and Sarmiento (1985)
Atmospheric CO_2	280 ppmV	275 ppmV	Petit et al. (1999)
Deep O_2	195 μmol/kg	191 μmol/kg	GEOSECS
Atmospheric $\delta^{13}C$	-6.5 ‰	-6.07 ‰	Toggweiler and Sarmiento (1985)
Southern Polar Ocean $\delta^{13}C$	0.6 ‰	0.6 ‰	Toggweiler and Sarmiento (1985)

VIII. Results and Discussion

Just as in the Stephens and Keeling study, the sensitivities of atmospheric carbon dioxide, deep water O_2 concentration and high-latitude southern ocean surface water $\delta^{13}C$ concentration to the effect of increasing Antarctic sea ice coverage were tested. In addition to Stephens and Keeling's results, the sensitivities of $\Delta^{14}C$ concentrations for the atmosphere, deep ocean and southern polar ocean were examined as well as the $\Delta^{14}C$ ages of the deep ocean and warm surface ocean.

The growth of the Antarctic ice sheet was simulated by reducing the piston velocity to see if Stephens and Keeling's results were reproducible using the four-box ocean model. For each of the four-box model runs, the carbonate ion was kept constant at 77 μmol/kg by dissolving or precipitating $CaCO_3$ to insure that the oceanic $CaCO_3$ budget is kept in balance. Figures 9 through 14 show the sensitivities of these parameters to the growth of Antarctic sea in the southern polar ocean.

Sensitivities: Atmospheric Carbon Dioxide

As shown in figure 9, reducing the piston velocity to zero in the southern polar ocean (which is equivalent to total ice coverage over this area), was not able to produce the large decrease in atmospheric CO_2 that was shown by Stephens and Keeling's model. The sensitivity of atmospheric CO2 to the piston velocity was significant only in the extreme case, when the ice sheet would have completely covered the southern polar ocean. Stephens and Keeling's sensitivities also show this type of behavior, however, their sensitivities are plotted on a log scale which exaggerates the actual sensitivity of atmospheric CO2 to increases in ice sheet growth. Furthermore, the surface area of southern polar ocean in the four-box ocean model is much greater than the surface area used by Stephens and Keeling, so the expected decrease of atmospheric CO_2 for the four-box model should be greater than the decrease produced by the Stephens and Keeling model. The observed glacial values and Stephens and Keeling's glacial values, with the exception of CO_2, best agree with the four-box model when the piston velocity is reduced to zero. Appendix C contains the steady-state solution for this glacial ocean scenario.

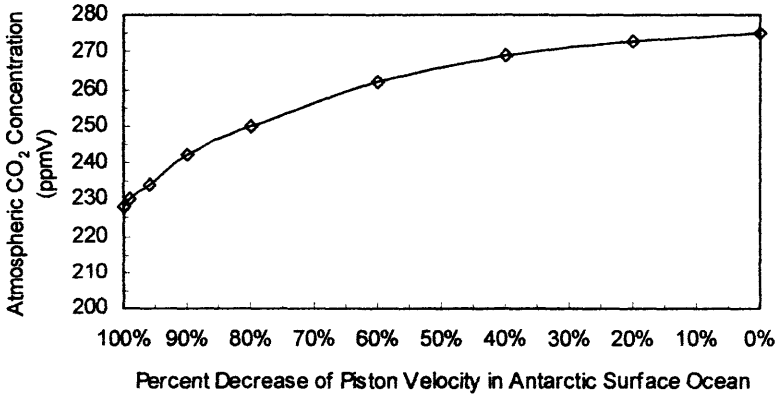

Figure 9: Sensitivity of Atmospheric CO_2

Sensitivities: Deep Ocean Oxygen and $\delta^{13}C$ Concentration

The sensitivity of deep oxygen for the four-box ocean model behaved similarly to Stephens and Keeling's model. Deep oxygen was not sensitive to limitations in air-sea gas exchange in the southern polar ocean until there was approximately 90% ice coverage. However, the quantitative amount of deep oxygen was lower for the four-box ocean model than for the Stephens and Keeling model. The southern polar surface $\delta^{13}C$ values for the four-box ocean model did not agree with the Stephens and Keeling values. In the four-box ocean model, $\delta^{13}C$ increased with the decrease of gas exchange. This difference is due to the fact that Stephens and Keeling included an input of 500 gigatons of terrestrial carbon (Stephens and Keeling, 2000). Figures 10 and 11 show the sensitivities of deep O_2 and $\delta^{13}C$.

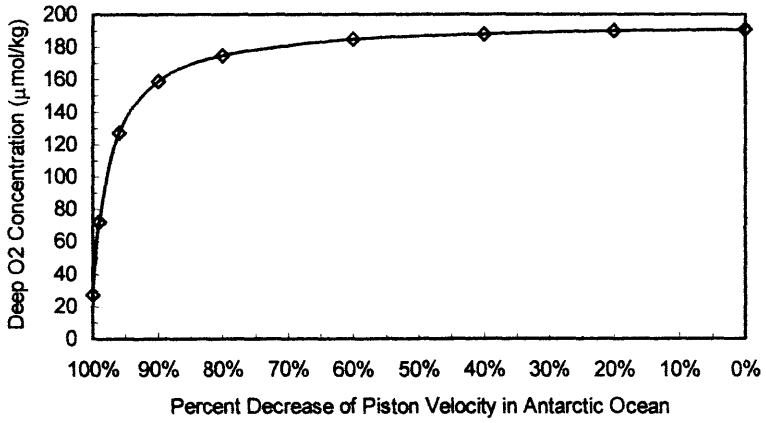

Figure 10: Sensitivity of Deep Oxygen

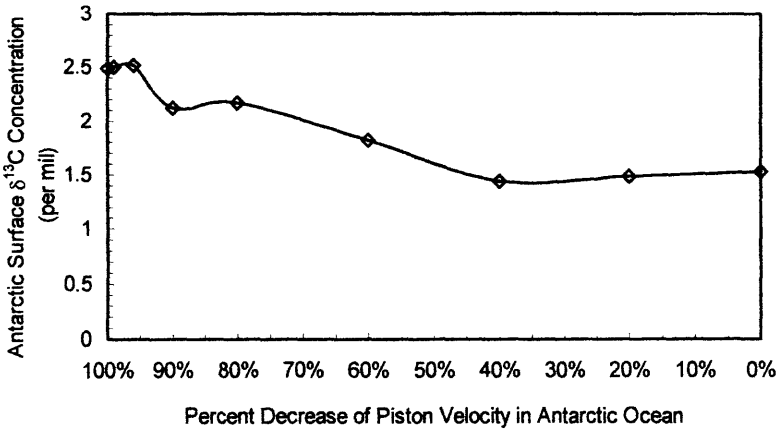

Figure 11: Sensitivity of Antarctic Surface $\delta^{13}C$

Sensitivities: Carbon-14

The atmospheric $\Delta^{14}C$ values were also comparable to observational data. The absolute atmospheric $\Delta^{14}C$ concentration was approximately 100 per mil during the last glacial period (Broecker, 1995). From figure 12, when the air-sea gas exchange was decreased to zero in the southern ocean surface box, the $\Delta^{14}C$ value of the four-box model was 115.29 per mille. Also from figure 12, the difference between the $\Delta^{14}C$ concentration of the deep and the atmosphere is increasing as the ice sheet grows. As the deep ocean continues to be cut off from the atmosphere, the difference would become larger.

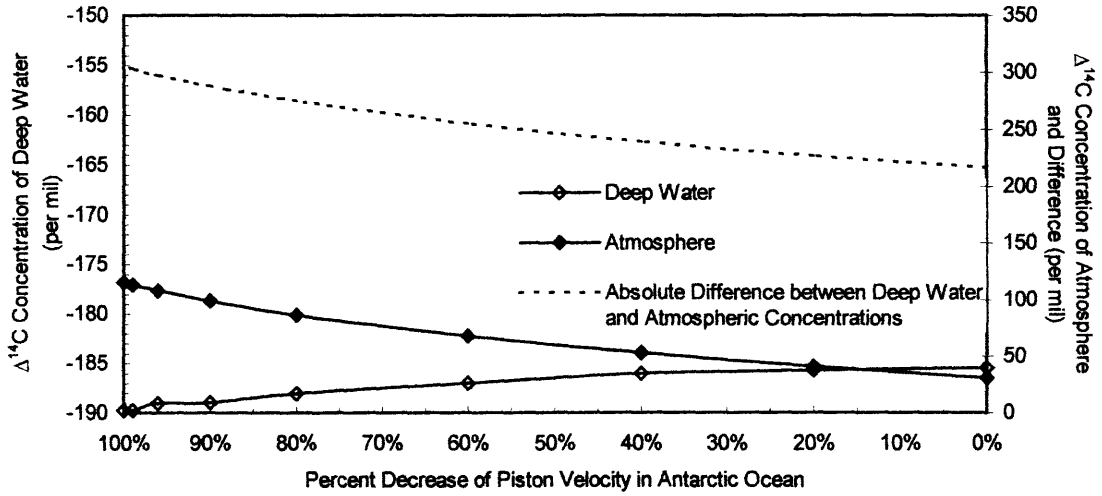

Figure 12: Sensitivity of absolute atmospheric and deep ocean $\Delta^{14}C$ concentration

Of particular interest is the behavior of $\Delta^{14}C$ in the southern polar ocean with respect to the $\Delta^{14}C$ concentration of the deep ocean. For the pre-industrial solution, the $\Delta^{14}C$ in the southern and deep ocean is significantly less than (approximately one-half) that of the $\Delta^{14}C$ found in the warm surface ocean and the northern polar ocean. Because input of carbon-14 into the ocean only occurs through interaction with the atmosphere, sequestered deep ocean water contains the lowest $\Delta^{14}C$ concentration (Broecker et al., 1990). As this water upwells into the southern ocean, the amount of $\Delta^{14}C$ slightly increases in the southern polar ocean due to the airing of the deep water with the atmosphere (Broecker et al., 1990).

In the best-guess glacial solution, when the southern polar ocean has been entirely cut off from interaction with the atmosphere, the $\Delta^{14}C$ concentration of the southern polar

ocean decreases further. The difference between the $\Delta^{14}C$ concentration of the deep ocean and the southern polar ocean decreases as upwelled deep water in the southern polar ocean sinks again to become Antarctic Bottom Water (AABW) with no interaction with the atmosphere. This already carbon-14 deficient AABW water is then mixed with the deep ocean.

Figure 13 shows this decrease in the concentration of $\Delta^{14}C$ value for the southern polar ocean as the piston velocity is reduced. Note that the concentrations of $\Delta^{14}C$ in the southern polar ocean and the deep ocean appear to be converging. When there is less gas exchange allowed in the southern polar ocean, it should behave as the deep ocean does. With no additional input of carbon-14 from the atmosphere and continued upwelling of lower $\Delta^{14}C$ from the deep ocean, the $\Delta^{14}C$ concentration of the two boxes should appear to agree as the gas exchange becomes more limited in the southern polar ocean.

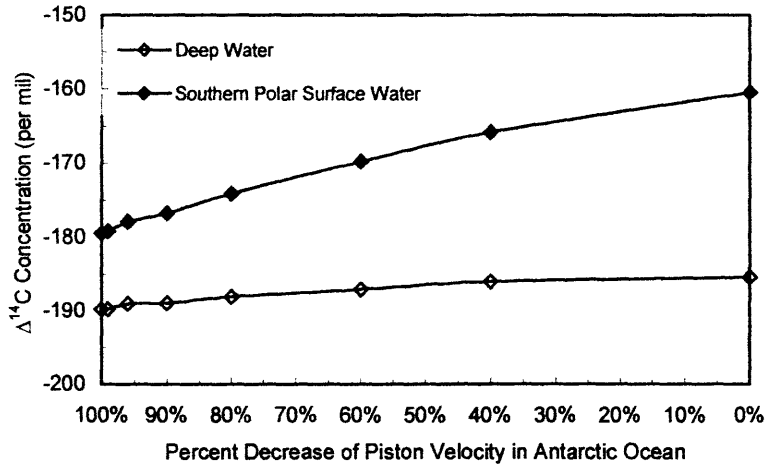

Figure 13: Sensitivity of southern polar and deep ocean $\Delta^{14}C$ concentration. Note that the $\Delta^{14}C$ of deep water is not sensitive to changes in the piston velocity. In addition, the $\Delta^{14}C$ concentrations appear to be converging.

By limiting the input of carbon-14 from the atmosphere into the southern polar ocean, the $\Delta^{14}C$ age of the deep water would also 'appear' older than for the pre-industrial solution. Figure 14 shows the increase in age of the deep water as the piston velocity is decreased. Figure 14 also shows the difference between the age of warm surface water and the age of the deep water as air-sea gas exchange is limited. As the deep ocean is prevented from interacting with the atmosphere, there is no additional input

of carbon-14 and $\Delta^{14}C$ further decreases. However, the warm surface ocean is still able to interact with the atmosphere and the difference between the age of the deep ocean and the age of the warm surface ocean becomes greater.

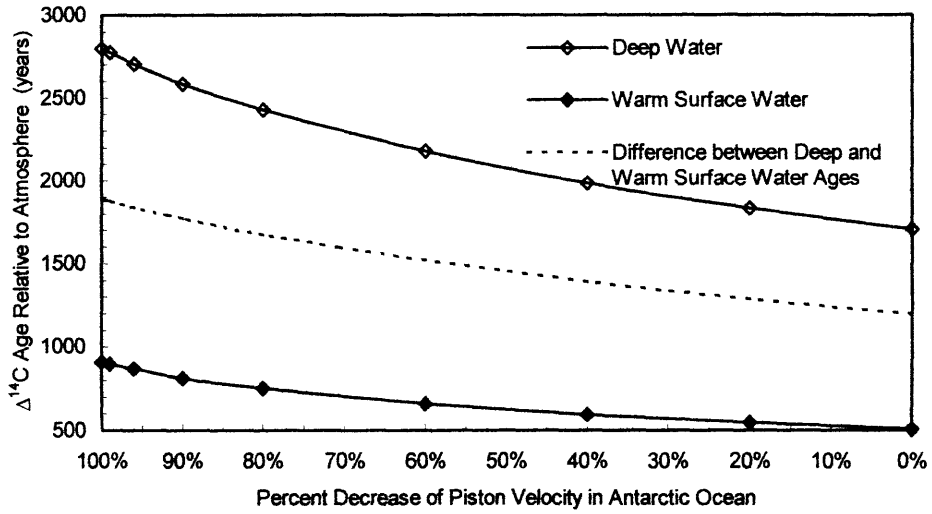

Figure 14: Sensitivity of $\Delta^{14}C$ age of the deep and warm surface ocean.

Other Methods to Reduce Atmospheric Carbon Dioxide

Since reducing the piston velocity in the four-box ocean model was not sensitive enough to produce large decreases in atmospheric CO_2, another hypothesis for the decrease of atmospheric CO_2 was tested using the four-box ocean model. As the gas exchange in the southern ocean was limited, dissolved CO_2 would have increased (Broecker and Peng, 1982). Increased CO_2 in the southern polar ocean would have increased biological productivity in the southern ocean and the phosphorus concentration in the southern ocean surface box would have decreased.

This hypothesis was tested using the four-box and three-box ocean models to see if they produced the same results as limiting the gas exchange in the southern polar ocean. Increased biological productivity was simulated by reducing the phosphorus concentration in the southern ocean polar box and polar box. To compare the three-box and four-box model results, the average preformed phosphate of the northern and southern polar oceans was calculated for the four-box ocean model using equation (18).

$$\text{Average Preformed Phosphate} = \left([P_2] + [P_4]\right) - \frac{360 - [O_{2_3}]}{RR_{O2}} \qquad (18)$$

where, P_a = phosphorus concentration in box *a*
O_{23} = concentration of oxygen in the deep ocean
RR_{O2} = Redfield ratio of P:O_2

For the four-box ocean model, when the phosphorus concentration was decreased in the southern ocean without limiting the air-sea gas exchange, atmospheric CO_2 also decreased. For a decrease of about one-third of the pre-industrial concentration of phosphorus in the southern polar ocean, the four-box ocean model produced an atmospheric CO_2 concentration of 210 ppmV. Figure 15 presents the sensitivities of atmospheric CO_2 to biological productivity in the southern ocean. Figure 16 presents the sensitivity of atmospheric CO_2 to changes in the polar phosphorus concentration using the Toggweiler and Sarmiento model. For both the three- and four-box models, increasing biological productivity in the polar ocean is a more effective means to reduce atmospheric CO_2 than limiting the air-sea gas exchange.

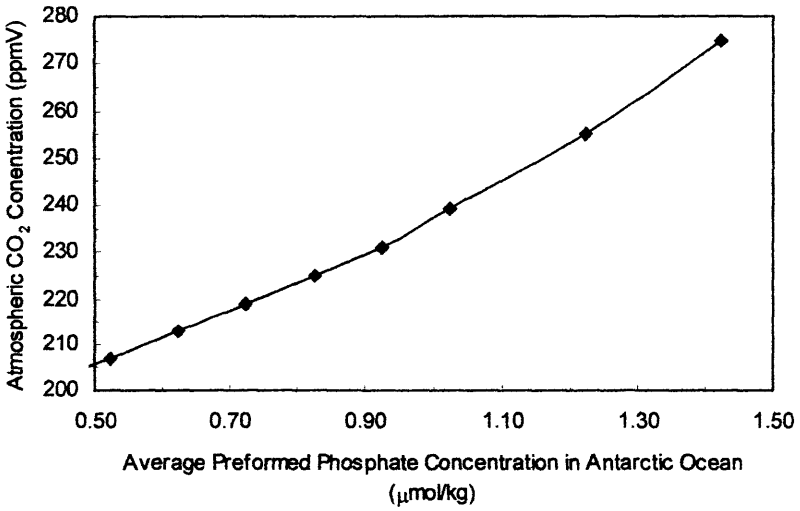

Figure 15: Sensitivity of atmospheric CO2 to increasing biological productivity in the southern polar ocean using the four-box ocean model.

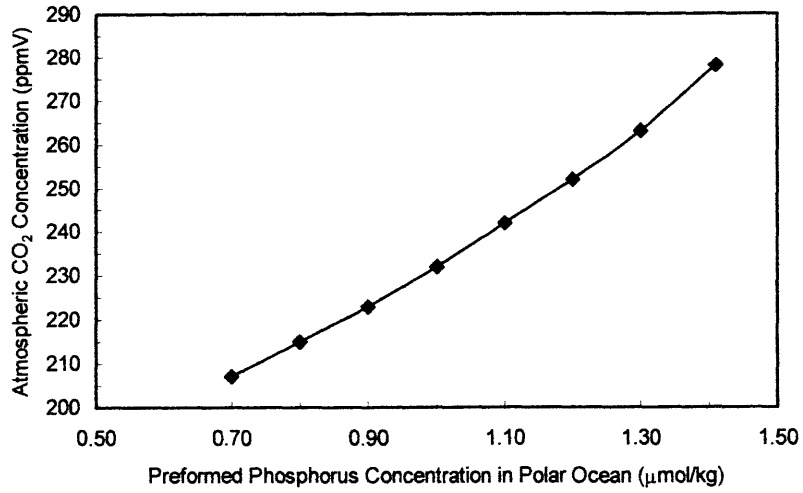

Figure 16: Sensitivity of atmospheric CO_2 to increasing biological productivity in the southern polar ocean using the three-box ocean model.

IX. Conclusions

The four-box ocean model was not sensitive enough to the growth of ice to produce the large decrease in atmospheric CO_2 that was shown in Stephens and Keeling's model. Both the six- and four-box models only showed a high-degree of sensitivity to the growth of the ice sheet when the coverage is very large. Carbon-14 was also calculated for the four-box ocean model, which was not examined in the six-box ocean model. The best-guess glacial condition for four-box ocean model, when only the piston velocity was changed, would be the case where the air-sea gas exchange was zero, or where there was total ice coverage, in the southern polar box. This steady-state solution is shown in Appendix C. In this case, the behavior is consistent with observational data, particularly for carbon-14, which was not calculated in the six-box ocean model. However, it may be unrealistic to assume that air-sea gas exchange in the southern ocean was zero during the last glacial period and, if that were the case, the sensitivity of atmospheric CO_2 concentration is still not as large when compared to the behavior of observed concentrations of atmospheric CO_2 during the last glacial period.

These results indicate that solely limiting gas exchange in the southern polar ocean due to ice coverage may not fully explain the reason that atmospheric CO_2 decreased during the last glacial period. Other mechanisms need to be explored in conjunction with

the growth of sea ice such as the lowering of phosphorus in the southern polar ocean, whose behavior indicates that atmospheric CO_2 concentrations in the four-box and three-box ocean models are more sensitive to changes in biological productivity than ice sheet growth.

Appendix A. Table of Constants Used in Four-Box Model †

Constant	Value	Units
Total Mass of the Ocean	1.29×10^{21}	kg
Total Area of the Ocean	3.45×10^{14}	m^2
Mole Volume of the Atmosphere	1.80×10^{20}	mol
Total Salinity in the Ocean	4.48×10^{22}	psu
Total Phosphorus in the Ocean	2.70×10^{21}	μmol
Total Alkalinity in the Ocean	3.06×10^{24}	μeq
Total Carbon in the Ocean	2.96×10^{24}	μmol
Total Carbon-13 in the Ocean	3.0×10^{22}	μmol
Kinetic Effect of Carbon-13	0.9988	-----
Kinetic Effect of Carbon-14	0.9976	-----
Production of Carbon-14 by Cosmic Rays	374.5	mol y^{-1}
$^{13}C/^{12}C$ Ratio	1.42×10^{-2}	-----
$^{14}C/^{12}C$ Ratio	1.18×10^{-12}	-----
Piston Velocity for Carbon	1080	m yr^{-1}
Piston Velocity for Oxygen ‡	1108	m yr^{-1}
Redfield Ratio of Alk:P	50	μmol μmol^{-1}
Redfield Ratio of Organic C:P	137.5	μmol μmol^{-1}
Redfield Ratio of O_2:P †	-175	μmol μmol^{-1}

†Values of constants are from the Toggwieler and Sarmiento (1985) model, unless otherwise noted.
‡ Broecker and Peng, 1982
† Broecker et al., 1985

Appendix B. Four-Box Ocean Model Solution for a Modern Pre-industrial Ocean

	Box 1: Warm Surface Ocean	Box 2: North Polar Ocean	Box 3: Deep Ocean	Box 4: South Polar Ocean	Atmosphere	Units
Water flux from Box 1 to	—	19	1	4		Sv
Water flux from Box 2 to	6	—	21	—	—	Sv
Water flux from Box 3 to	1	7	-----	67	—	Sv
Water flux from Box 4 to	19	—	53	—	—	Sv
Tropical Flux from Box 1 to	—	1	—	1	—	Sv
Temperature	20	2.5	2	2.5	—	°C
Salinity	37.44	35.33	34.64	34.32	—	
Phosphorus	0.2	0.69	2.1	1.7	—	μmol/kg
Phosph. Part. Flux to Box 3	0.004	0.000	-----	0.026	—	mol/m²/yr
Alkalinity	2467	2349	2367	2338	—	μeq/kg
Normalized Alkalinity	2306	2327	2391	2385	—	mol/m²/yr
Alk. Part. Flux to Box 3	0.182	0.001	-----	0.106	—	mol/m²/yr
Carbon	2081	2123	2258	2161	—	μmol/kg
Normalized Carbon	1945	2104	2281	2204	—	μmol/kg
Carbon Part. Flux to Box 3	0.591	0.020	-----	3.247	—	mol/m²/yr
pCO_2	277	236	-----	303	275	ppmV
Piston Velocity	1080	1080	-----	1080	—	m/yr
% Chng in Piston Velocity	0	0	-----	0	—	--
Carbonate Ion CO_3^{2-}	281	164	77	134	—	mol/kg
$^{13}CO_2$	23.84	24.31	25.83	24.73	—	μmol/kg
$\delta^{13}C$	2.24	1.87	0.68	1.52	-6.08	per mille
$p^{13}CO_2$	3.15	2.67	-----	3.43	3.13	ppmV
$^{13}CO_2$ Part. Flux to Box 3	0.007	0.000	-----	0.036	—	mol/m²/yr
$^{14}CO_2$	2.58	2.56	2.34	2.31	—	fmol/kg
$\delta^{14}C$	25.13	-1.19	-141.34	-113.49	71.09	per mille
$p^{14}CO_2$	0.34	0.28	-----	0.32	0.36	fmol/mol
$\Delta^{14}C$	-30.73	-54.86	-185.44	-160.52	30.55	per mille
^{14}C age	508	717	1955	1704	986**	years
$^{14}CO_2$ Part. Flux to Box 3	168.81	0.50	-----	79.92	—	mol/kg
O_2	223	322	191	322	—	μmol/kg
O_2 Part. Flux to Box 3	-0.64	-0.03	-----	-4.62	—	mol/m²/yr
O_2 Piston Velocity	1104	1104	-----	1104	—	m/yr

**NOTE: This is NOT the age of atmosphere; this is the residence time of deep water in the ocean. For pre-industrial conditions, the value should be approx. 1000 years.

Constants	Value	
% Chng in total Phosphorus	0	
Total Phosphorus of Ocean	2.7E+21	μmol
CaCO3 Adjustment	0	
Total Alkalinity of Ocean	3.06E+24	μmol
Organic Carbon Adjustment	0	
Total Carbon in Ocean	2.961E+24	μmol

Redfield Ratio for	Box 1	Box 2	Box 4
Alkalinity	50	4	4
Organic CO_2	137.5	121	121
ΣCO_2	162.5	123	123
$^{13}CO_2$	1.83	1.37	1.37
$^{14}CO_2$	0.16	0.12	0.12
O_2	-175	-175	-175

Appendix C. Four-Box Ocean Model Best-Guess Solutions for a Glacial Ocean by Limiting the Air-Sea Gas Exchange for the Southern Polar Ocean.

	Box 1: Warm Surface Ocean	Box 2: North Polar Ocean	Box 3: Deep Ocean	Box 4: South Polar Ocean	Atmosphere	Units
Water flux from Box 1 to	—	19	1	4		Sv
Water flux from Box 2 to	6	—	21	—	—	Sv
Water flux from Box 3 to	1	7	—	67	—	Sv
Water flux from Box 4 to	19	—	53	—	—	Sv
Tropical Flux from Box 1 to	—	1	—	1	—	Sv
Temperature	20	2.5	2	2.5	—	°C
Salinity	37.44	35.33	34.64	34.32	—	
Phosphorus	0.2	0.69	2.1	1.7	—	umol/kg
Phosph. Part. Flux to Box 3	0.004	0.000	—	0.026	—	mol/m²/yr
Alkalinity	2475	2357	2375	2346	—	ueq/kg
Normalized Alkalinity	2314	2335	2399	2393	—	mol/m²/yr
Alk. Part. Flux to Box 3	0.182	0.001	—	0.106	—	mol/m²/yr
Carbon	2045	2091	2266	2185	—	umol/kg
Normalized Carbon	1912	2072	2269	2229	—	umol/kg
Carbon Part. Flux to Box 3	0.591	0.020	—	3.247	—	mol/m²/yr
pCO_2	232	192	—	337	227	ppmV
Piston Velocity	1080	1080	—	0	—	m/yr
% Chng in Piston Velocity	0	0	—	-1	—	--
Carbonate Ion CO_3^{2-}	312	190	77	124	—	mol/kg
$^{13}CO_2$	23.49	24.00	25.96	25.05	—	umol/kg
$\delta\,^{13}C$	5.02	4.40	2.31	2.92	-2.95	per mille
$p\,^{13}CO_2$	2.65	2.18	—	3.83	2.58	ppmV
$^{13}CO_2$ Part. Flux to Box 3	0.007	0.000	—	0.036	—	mol/m²/yr
$^{14}CO_2$	2.65	2.62	2.35	2.29	—	fmol/kg
$\delta\,^{14}C$	71.61	38.54	-142.96	-130.89	166.37	per mille
$p\,^{14}CO_2$	0.30	0.24	—	0.35	0.32	fmol/mol
$\Delta\,^{14}C$	7.28	-22.52	-189.77	-179.42	114.93	per mille
^{14}C age	915	1188	2920	2601	1613**	years
$^{14}CO_2$ Part. Flux to Box 3	168.31	0.50	—	79.68	—	mol/kg
O_2	222	321	27	90	—	umol/kg
O_2 Part. Flux to Box 3	-0.64	-0.03	—	-4.62	—	mol/m²/yr
O_2 Piston Velocity	1104	1104	—	0	—	m/yr

**NOTE: This is NOT the age of atmosphere; this is the residence time of deep water in the ocean. For pre-industrial conditions, the value should be approx. 1000 years.

Constants	Value	
% Chng in total Phosphorus	0	
Total Phosphorus of Ocean	2.7E+21	umol
CaCO3 Adjustment	4	
Total Alkalinity of Ocean	3.07034E+24	umol
Organic Carbon Adjustment	0	
Total Carbon in Ocean	2.961E+24	umol

Redfield Ratio for	Box 1	Box 2	Box 4
Alkalinity	50	4	4
Organic CO_2	137.5	121	121
ΣCO_2	162.5	123	123
$^{13}CO_2$	1.83	1.37	1.37
$^{14}CO_2$	0.16	0.12	0.12
O_2	-175	-175	-175

Works Cited

Broecker W.S., Virgilio, A. and Peng, Th., 1991, Radiocarbon age of waters in the deep Atlantic revisited, *Geophysical Research Letters*, 18(1), 1-3.

Broecker, W.S. and Peng, Th., 1982, *Tracers in the Sea*. Eldigio Press, Palisades, NY. 660 pp.

Broecker et al., 1990, The distribution of radiocarbon in the glacial ocean, *Global Biogeochemical Cycles*, 4(1), 103-117.

Broecker, W.S., 1995, *The Glacial World According to Wally*. Eldigio Press, Palisades, NY. 318 pp.

Broecker, W.S., Takahashi, T., and Takahashi, T., 1985, Sources of flow patterns of deep waters as deduced from potential temperature, salinity, and initial phosphate concentration, *Journal of Geophysical Research*, 90, 6907-6924.

Broecker, W.S., 1991, The great ocean conveyor, *Oceanography*, 4(2), 79-89.

Chester R., 1990, *Marine Geochemistry*. Unwin Hymen, London, England. 698 pp.

Geochemical Ocean Sections Study, a global survey of the three-dimensional distribution of chemical, isotopic, and radiochemical tracers in the ocean. The expeditions were in the Atlantic from July 1972 to May 1973; the Pacific from August 1973 to June 1974, and the Indian Ocean from December 1977 to March 1978.

Knox, F. and McElroy, M, 1984, Changes in atmospheric CO2: The influence of marine biota at high latitudes, *Journal of Geophysical Research*, 89, 4629-4637.

Petit, J.R. and 18 others, 1999, Climate and atmospheric history of the past 420,000 years from the Vostok core, Antarctica, *Nature*, 399, 429-436.

Pilson, M., 1998, *An Introduction to the Chemistry of the Sea*. Simon and Schuster, New Jersey. 431 pp.

Toggweiler, J.R. and Sarmiento, J.L. *Glacial to Interglacial Changes in Atmospheric Carbon Dioxide: The Critical Role of Ocean Surface Water in High Latitudes*. In The Carbon Cycle and Atmospheric CO2: Natural Variations Archaen to Present (ed. E.A.S.a. W.S. Broecker), Vol. 32, pp. 163-184. Am. Geophys. Union.

Siegenthaler, U. and Wenk, Th., 1984, Rapid atmospheric CO_2 variations and ocean circulation, *Nature*, 308, 624-626.

Sigman, D. and Boyle E., 2000, Glacial-Interglacial variations in atmospheric carbon dioxide, *Nature*, 407, 859-869.

Stephens B. and Keeling R., 2000, The influence of Antarctic sea ice on glacial-interglacial CO2 variations, *Nature*, 404, 171-174.